60 MeV Proton Irradiation Effects on NO-Annealed and Standard-Oxide Deep Submicron MOSFETs

Eddy Simoen, Jan Hermans, Abdelkarim Mercha, Wim Vereecken, Carl Vermoere, Cor Claeys, *Senior Member, IEEE*, Emmanuel Augendre, Gonçal Badenes, *Senior Member, IEEE*, and Ali Mohammadzadeh

***Abstract*—The impact of 60 MeV proton irradiation on the static device parameters of CMOS transistors fabricated in a 0.18 μm technology is reported and studied as a function of the polysilicon gate length L_{poly}. In addition, the role of the gate dielectric in the radiation response of the threshold voltage, the transconductance, the subthreshold swing, the series resistance and the Gate-Induced Drain Leakage (GIDL) current is investigated. For certain parameters, an anomalous length dependence has been observed. Furthermore, a stronger degradation is found for the transistors with an NO-annealed gate dielectric compared with a standard thermal gate oxide. Combining the charge separation technique with the GIDL current, additional insight in the damage mechanisms is gained. It is shown that there is evidence for electron trapping close to the drain in the case of the NO devices**

***Index Terms*—MOSFETs, protons, radiation effects, radiation hardening.**

I. INTRODUCTION

One of the roadblocks on the way to scaling CMOS is the gate oxide thickness, reaching the tunneling limit for next generations of technologies. Ultimately, the gate oxide will have to be replaced by a high-*k* dielectric, but as an intermediate step, nitrided or reoxidised nitrided oxides can be useful. The use of nitrided oxides brings along certain advantages with respect to gate oxide reliability and boron penetration. On the other hand, it is known that the presence of N atoms close to the interface introduces fixed oxide charges, which reduce the mobility and transconductance at low to intermediate gate voltage V_{GS} [1]-[3]. It has also been reported that a higher radiation tolerance can be achieved under certain gate processing conditions [2], although this has not been verified thoroughly for ultra-thin gate oxides.

From a radiation damage viewpoint, scaling offers only but advantages at first sight (see [4] and References therein). This is tightly connected to the fact that below the tunneling limit, essentially no holes are permanently trapped in a thin oxide (t_{ox}<6 nm) [5], while at the same time, it has been observed that the radiation-induced density of interface traps ΔN_{it} reduces according to a power law with t_{ox} [6]. However, for higher radiation doses/fluences some new degradation phenomena have been observed in ultra-thin gate dielectrics, which are a potential source of concern [4],[7],[8]. In addition, it has recently been observed that radiation-induced dopant deactivation in the silicon substrate may contribute to the change of the device parameters [9]-[11]. From high-energy particle irradiation studies of shallow n^+p junctions fabricated in a B-doped p-well, it was concluded that displacement damage plays a direct role in the dopant deactivation [12],[13]. As the near surface doping density is critical for the control of the short-channel effects, one can imagine that MOSFETs suffer from such a degradation mechanism.

It is the aim of this paper to investigate the impact of 60 MeV proton irradiations on the behaviour of deep submicron MOSFETs fabricated in a 0.18 μm CMOS technology. The device parameters: the threshold voltage V_T, the transconductance g_m, the subthreshold swing S and the series resistance R_s will be studied as a function of the device length. Devices with an NO-annealed oxide will be compared with standard thermal oxide gates. Evidence is given for the creation of both oxide and interface charges after the proton irradiation, whereby the NO-annealed devices show a stronger degradation.

II. EXPERIMENTAL

The transistors have been fabricated in a 0.18 μm CMOS technology using a Polysilicon Encapsulated Local Oxidation of Silicon (PELOX) isolation scheme. Standard thermal oxide MOSFETs (abbreviated OX) received a wet oxidation at 650 ^oC, while the NO devices were first dry oxidised at 850 ^oC, followed by a 30 min NO anneal at the same temperature. In both cases the gate dielectric thickness was 3.5 nm. For the standard thermal oxide transistors, a boron implantation was used for the fabrication of the source-drain junctions of the p-MOSFETs. For the NO p-MOSFETs, a BF_2 implantation could be performed, as the presence of the nitrogen suppresses sufficiently the B penetration, which is enhanced by the presence of F. The relevant process information is summarised in Table I. Devices coming from one wafer per split have been studied here.

Meanwhile, a detailed characterisation of the interface and oxide quality of the OX and NO devices has been undertaken, combining charge pumping measurements on L=10 μm, W=10 μm single transistors for the extraction of the density of interface traps (D_{it}) and low-frequency (LF) noise measurements in the ohmic regime, at relatively low gate overdrive on L=2 μm, W=10 μm MOSFETs [14]. The noise analysis results in a density of oxide traps (D_{ot}). As can be seen from the data of Table IIa and IIb, the presence of

Eddy Simoen, Jan Hermans, Abdelkarim Mercha, Emmanuel Augendre, Cor Claeys and Gonçal Badenes are with IMEC, Kapeldreef 75, B-3001 Leuven, Belgium.

Wim Vereecken, Carl Vermoere and Cor Claeys are with the E.E. Dept., KU Leuven, Kasteelpark Arenberg 10, B-3001 Leuven, Belgium.

Abdelkarim Mercha is on leave from the University of Caen (France).

Ali Mohammadzadeh is with ESTEC-ESA, Keplerlaan 1, NL-2200 AG Noordwijk, The Netherlands.

nitrogen has a tremendous impact on D_{ot} of the p-channel devices (and, hence, on the LF noise magnitude), while the interface properties before irradiation are far less affected. The higher noise for the NO p-MOSFETs can be explained by the fact that this parameter is particularly sensitive to the presence of nitrogen-related near interface oxide traps [14]. It should be remarked that the data quoted in Table II have been derived on several devices and should be considered as averages for the process split.

TABLE I
TECHNOLOGICAL PARAMETERS OF THE 0.18 μm CMOS TECHNOLOGY

Process step	Process parameter
Gate oxide thickness	3.5 nm
Gate oxidation OX	wet at 650ºC
Gate oxidation NO	dry at 850ºC+NO at 850ºC
Isolation	PELOX
Thickness field oxide	400 nm
p-well implantation	200 & 55 keV B
n-well implantation	380 (P) & 120 keV (As)
Nitride spacer	80 nm
Silicidation	Ti/Co (8/15 nm)

TABLE IIa
INTERFACE AND OXIDE TRAP DENSITY OF THE VIRGIN OX AND NO p-CHANNEL DEVICES

Gate Dielectric	D_{it} ($eV^{-1}cm^{-2}$) (L=10 μm)	D_{ot} ($eV^{-1}cm^{-2}$) (L=2 μm)
OX	$1.4x10^{11}$	$5.4x10^{10}$
NO	$8.9x10^{10}$	$4.1x10^{11}$

TABLE IIb
INTERFACE AND OXIDE TRAP DENSITY OF THE VIRGIN OX AND NO n-CHANNEL DEVICES

Gate Dielectric	D_{it} ($eV^{-1}cm^{-2}$) (L=10 μm)	D_{ot} ($eV^{-1}cm^{-2}$) (L=2 μm)
OX	$4.0x10^{10}$	$3.2x10^{10}$
NO	$4.1x10^{10}$	$8.5x10^{10}$

Transistors with a polysilicon (poly) gate length (L_{poly}) from 0.18 μm till 0.48 μm have been mounted in 24 pins dual-in-line packages for the proton irradiations. The gate width W was 10 μm. Unbiased 60 MeV proton irradiations were performed at the Cyclone cyclotron facility (Louvain-la-Neuve) for two fluences typical for space applications, i.e., $3x10^{10}$ and 10^{11} cm^{-2}. The latter fluence corresponds to an equivalent total dose of about 13.5 krad(Si). The contacts were left floating during the irradiation. Experience has learnt that for deep submicron technologies, this leads to the highest degradation (worst-case scenario). Testing was performed within 24 h after the exposure.

More details about the pre- and post irradiation device characterisation can be found in Ref. 15. Here, the focus is on a comparison of the behaviour of NO and OX components under a 60 MeV proton irradiation. For the first time, Gate-Induced Drain Leakage (GIDL) current data are reported on these devices. The effective device length and series resistance have been extracted using a modified Shift and Ratio (S&R) method [16], whereby the linear input curve of a long reference device, i.e., L=5 μm is combined with the one obtained for shorter lengths.

III. RESULTS

A. Threshold Voltage

As reported before [15], the OX n-MOSFETs show a kind of cross-over behaviour with L_{poly}, whereby the threshold voltage V_T becomes lower after proton irradiation for the long channels - which is normally expected for an n-MOSFET - while for the shortest device lengths just the opposite is observed in Fig. 1a and 1b. In contrast, for the NO counterparts the V_T decreases for all lengths both after the $3x10^{10}$ cm^{-2} (Fig. 2a) and the 10^{11} cm^{-2} (Fig. 2b) irradiation. The change in the threshold voltage is explicitly shown in Fig. 3a (OX) and 3b (NO).

As can be derived from Figs 2 and 3, the overall V_T shift is quite small, which is expected for deep submicron transistors [17]. In this respect, it should be remarked that the measurement accuracy is expected better than 1 %. For the NO devices, the V_T reduction increases monotonously with decreasing length, suggesting more net positive charge trap-

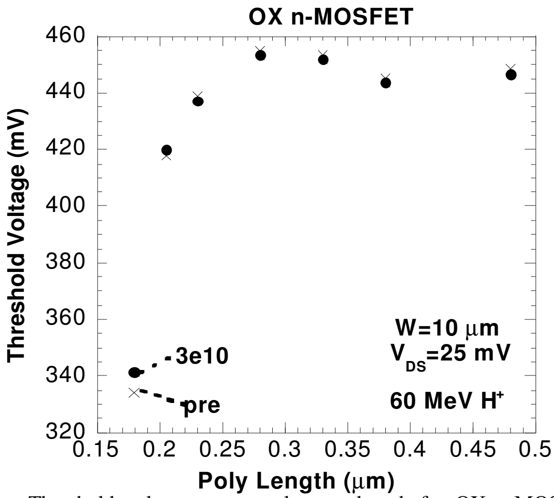

Fig. 1.a. Threshold voltage versus poly gate length for OX n-MOSFETs, before and after a $3x10^{10}$ cm^{-2} 60 MeV proton irradiation.

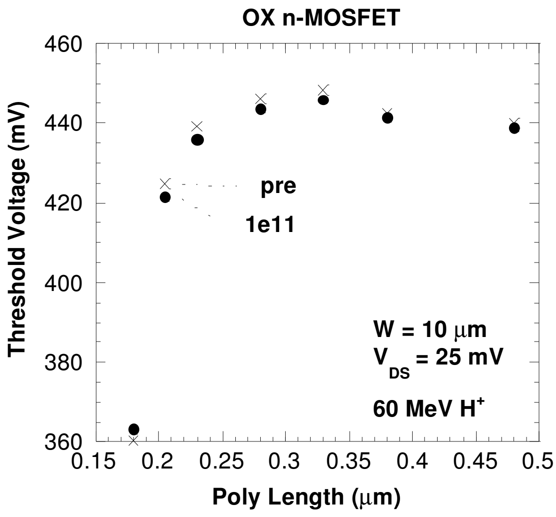

Fig. 1.b. Threshold voltage versus poly gate length for OX n-MOSFETs, before and after a 10^{11} cm^{-2} 60 MeV proton irradiation.

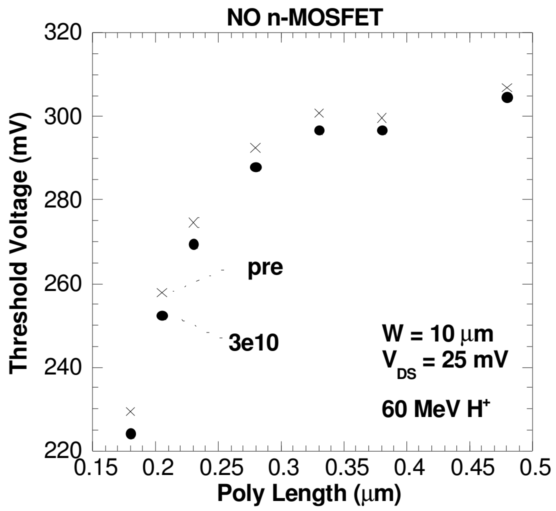

Fig. 2.a. Threshold voltage versus poly gate length for NO n-MOSFETs, before and after a $3x10^{10}$ cm^{-2} 60 MeV proton irradiation.

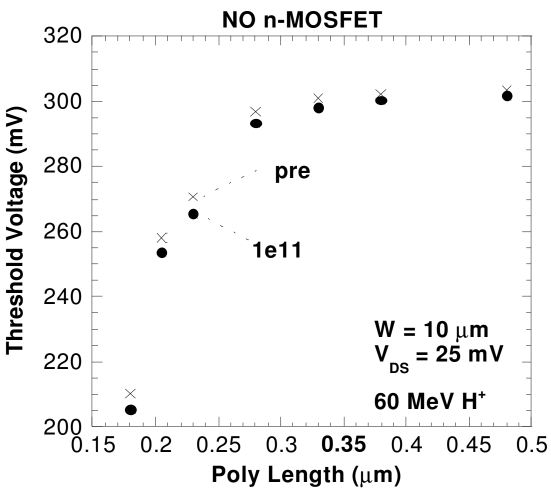

Fig. 2.b. Threshold voltage versus poly gate length for NO n-MOSFETs, before and after a 10^{11} cm^{-2} 60 MeV proton irradiation.

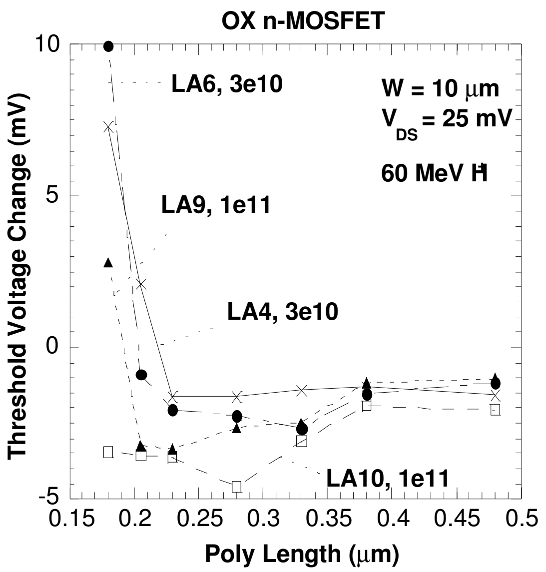

Fig. 3.a. Threshold voltage change after a 60 MeV proton irradiation for arrays of OX n-MOSFETs.

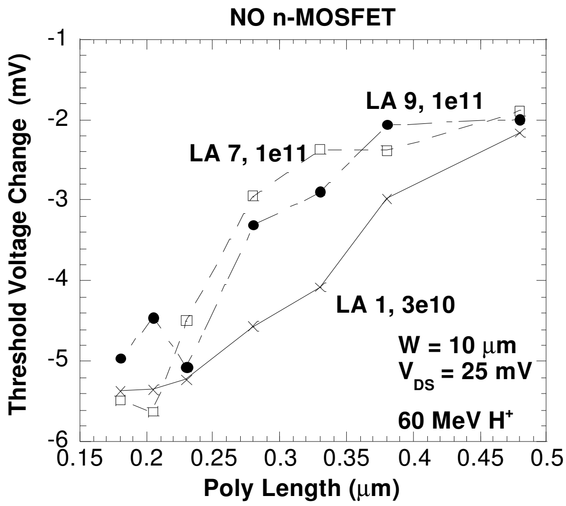

Fig. 3.b. Threshold voltage change after a 60 MeV proton irradiation for arrays of NO n-MOSFETs.

ping – if that is the degradation mechanism at stake. For the OX devices, the cross-over behaviour indicates a complex interplay between charge trapping in the oxide, interface-state creation and possible substrate contributions [15]. In other words, it is believed that besides degradation of the gate and spacer dielectrics, there exists a contribution from 60 MeV proton displacement damage in the substrate. The latter can lead to a change in the channel doping density and profile. The analysis of such an effect is, however, complicated by the fact that the lateral and vertical doping profile is largely non-uniform, owing to the application of Lowly-Doped Drain (LDD) implantations and a retrograde well, respectively. The present results confirm what has been previously reported on similar devices coming from different wafer splits of the same technology [15]. Moreover, similar trends have recently been derived for devices fabricated in IMEC's 0.13 μm CMOS technology, after biased 60 MeV proton irradiations.

The fluence (Φ) dependence of the V_T changes is rather anomalous, as there appears to be a kind of rebound behaviour. This is best noted for the NO devices shown in Fig. 3b, where the ΔV_T is smaller for the 10^{11} fluence compared with $3x10^{10}$ p/cm^2. The OX devices exhibit a tendency for more negative V_T shift for the larger fluence, especially for the shorter channel lengths (Fig. 3a). Generally speaking, the threshold voltage degradation of the NO and OX n-MOSFETs becomes more similar after the higher fluence proton exposure. It should finally be remarked that the V_T degradation of the p-MOSFETs is within the range ±2 mV, for both fluences studied. Furthermore, no clear trends with L_{poly} have been found [18]. Therefore, the remainder of the paper will focus on the degradation of the n-channel transistors.

B. Transconductance

Figure 4 compares the transconducance g_m before irradiation for a L_{poly}=0.18 μm n-MOSFET with OX and NO gate. As expected [1]-[3], the peak or maximum g_m is lower for the NO device, which is believed to be related to additional trapped charges in the oxide, close to the interface. This is in line with the D_{ot} data of Table IIb. Furthermore, the decrease in peak g_m is more pronounced for shorter channels.

On the other hand, at high gate overdrives (V_{GS}-V_T), a cross-over occurs, indicated in Fig. 4, whereby the g_m for the NO transistor becomes higher. In other words, the degradation of g_m with increasing vertical field is less in the NO case. According to the literature [1],[3], this behaviour can be explained by considering the effect of trapped electrons in the oxide, which repel the channel electrons, pushing them from the Si-SiO_2 interface. In this way, surface roughness scattering, dominant at high vertical fields, is less prominent in NO compared with OX devices.

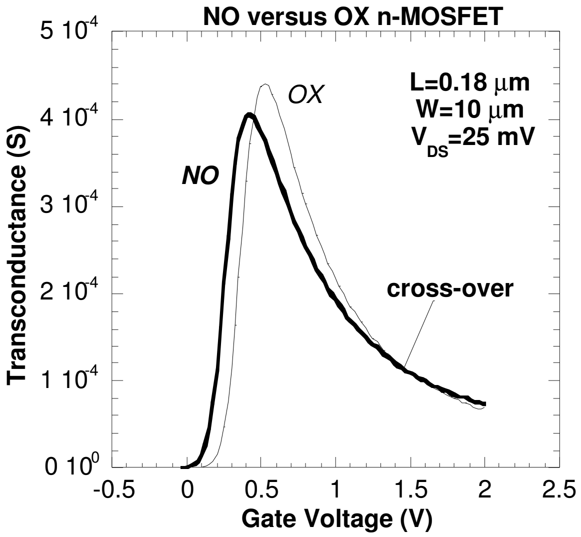

Fig. 4. Transconductance versus gate voltage in the ohmic regime for a L_{poly}=0.18 µm NO and OX n-MOSFET.

After proton irradiation, it is noted by comparing Fig. 4 with Fig. 5a (3x10^{10} p/cm^2) or Fig. 5b (10^{11} p/cm^2) that the maximum transconductance has become smaller. This is illustrated more explicitly in Fig. 6a and Fig. 6b, showing g_{mmax} versus the inverse poly length, before and after exposure to a 60 MeV proton fluence of 10^{11} cm^{-2}. The peak transconductance reduces with 3 to 13 % (OX) and with 1 to 9 % (NO) going from L_{poly}=0.48 µm to 0.18 µm. In other words, the degradation of g_m is less for the NO case compared with OX devices, both in absolute and relative value and shows, furthermore, a short-channel effect, whereby more severe damage is observed for the shorter transistors. In other words, the degradation becomes higher for shorter L's, while marginal changes are found for the long channel n-MOSFETs. From the high field behaviour of Fig. 5b, one may come to the conclusion that also there, NO suffers less severe degradation. At the same time, the g_m cross-over behaviour is shifted somewhat to higher V_{GS}, if Fig. 4 is compared with Fig. 5a or Fig. 5b. There seems to be a slight return of the cross-over point for the 10^{11} p/cm^2 fluence compared with the 3x10^{10} p/cm^2 case. This behaviour can not be explained by the radiation-induced shift in the threshold voltage, as ΔV_T is much smaller. A possible explanation could be that due to the trapped oxide/interface charge, the impact of surface roughness scattering is delayed to higher gate overdrives. Another important factor is the series resistance Rs, which increases more for the NO transistors, as will be seen below.

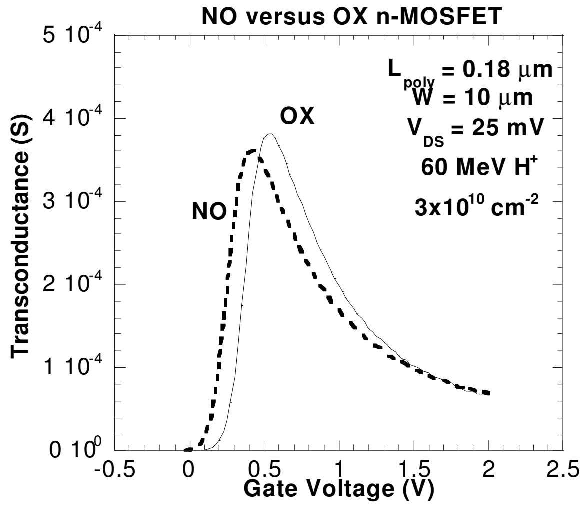

Fig. 5.a. Transconductance of a 0.18 µm NO and OX n-MOSFET after a 3x10^{10} cm^{-2} 60 MeV proton irradiation.

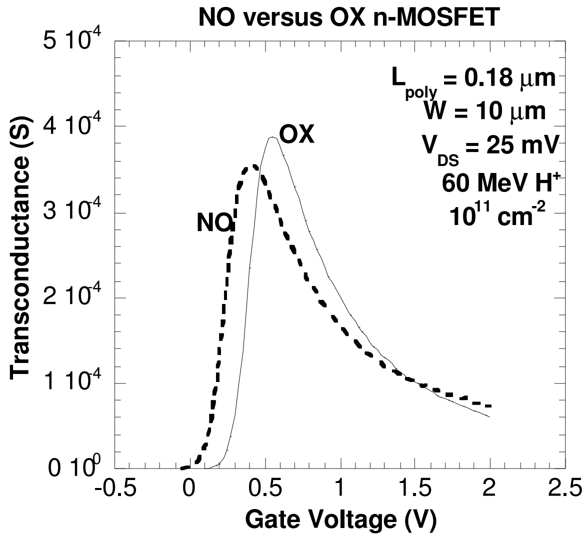

Fig. 5.b. Transconductance of a 0.18 µm NO and OX n-MOSFET after a 10^{11} cm^{-2} 60 MeV proton irradiation.

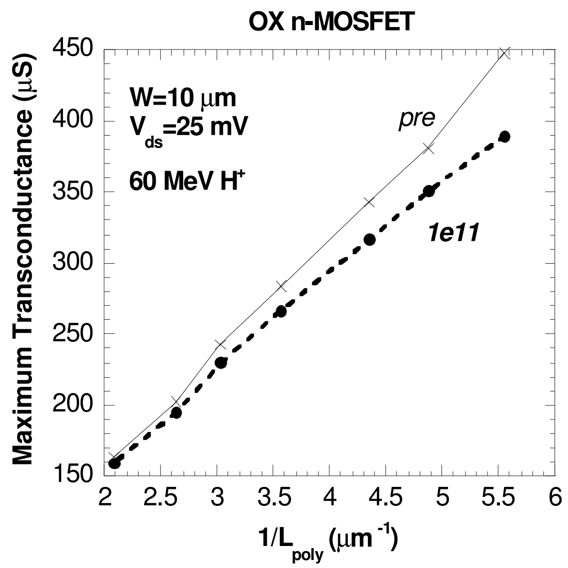

Fig. 6.a. Maximum transconductance versus inverse effective length for OX n-MOSFETs, after a 10^{11} cm^{-2} 60 MeV proton irradiation.

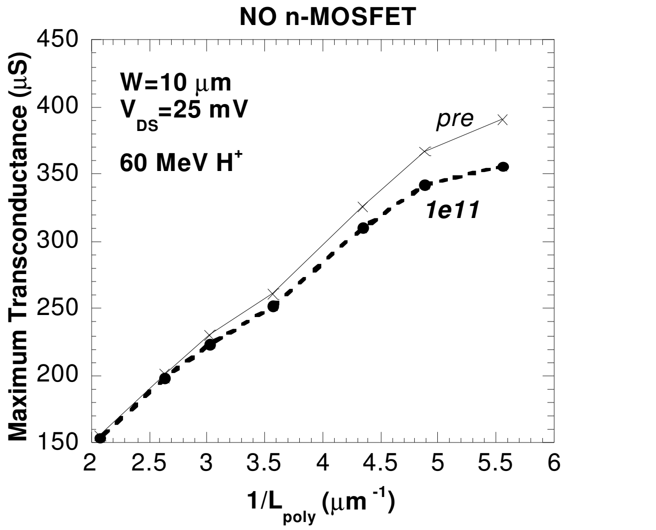

Fig. 6.b. Maximum transconductance versus inverse effective length for NO n-MOSFETs, after a 10^{11} cm^{-2} 60 MeV proton irradiation.

C. Subthreshold Swing

Interestingly, the subthreshold swing S also shows a kind of proton-radiation induced cross-over behaviour, as can be derived from Figs 7a (OX) and 7b (NO). Before exposure, S shows the classical short-channel increase with reducing length. It is slightly lower for OX compared with NO, which reflects the lower D_{it} of Table IIb. After 60 MeV protons and for both fluences, an increase of S is observed for OX devices, whereby ΔS is more pronounced for the longer transistors. On the other hand, a reduction of S is found for the long NO n-MOSFETs, while the opposite is seen for the shortest devices. The cross-over occurs at L_{poly}~0.22 μm for both fluences studied.

D. Series Resistance

Finally, from Fig. 8a and Fig. 8b, one can derive that the effective device length increases after proton irradiation. In addition, the series resistance R_s shown in Figs 9a and 9b becomes also higher. This increase is more pronounced for the NO devices. For the extraction a 5 μm 'long channel reference' has been used [18].

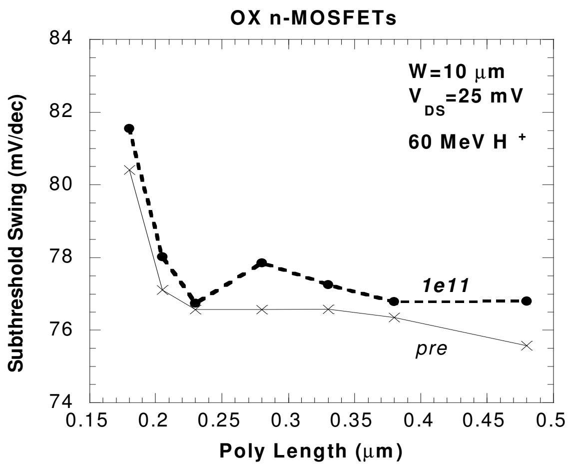

Fig. 7.a. Subthreshold swing versus L_{poly} before and after a 10^{11} cm^{-2} 60 MeV proton irradiation, corresponding with the OX split.

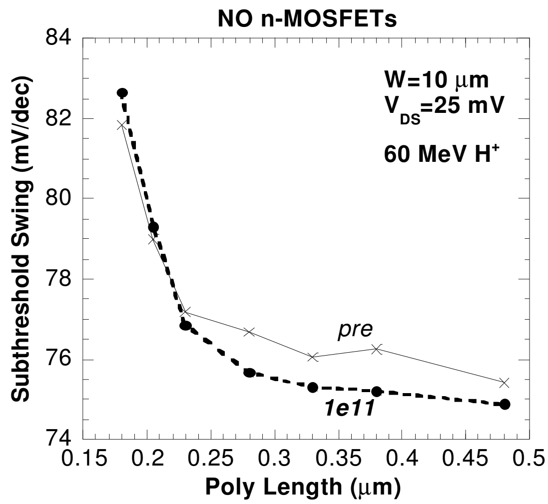

Fig. 7.b Subthreshold swing versus L_{poly} before and after a 10^{11} cm^{-2} 60 MeV proton irradiation, corresponding with the NO split.

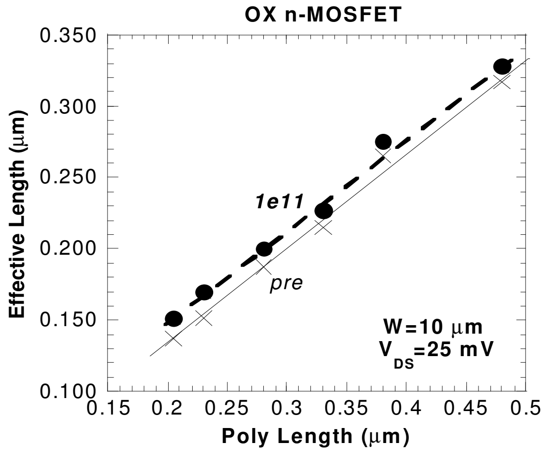

Fig. 8.a. Effective length versus poly length for OX n-MOSFETs before and after a 10^{11} cm^{-2} 60 MeV proton irradiation.

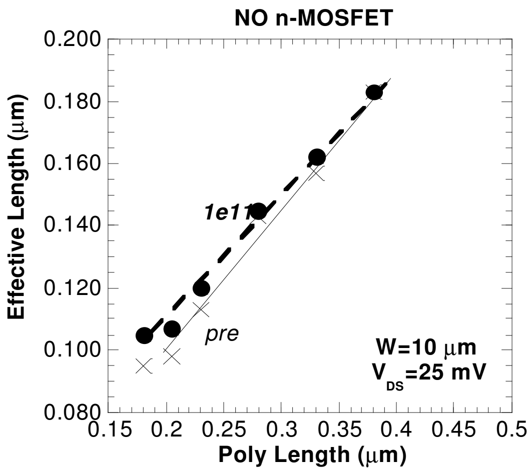

Fig. 8.b. Effective length versus poly length for NO n-MOSFETs before and after a 10^{11} cm^{-2} 60 MeV proton irradiation.

At first sight, it is difficult to understand this different R_s behaviour for NO and OX n-MOSFETs, as they have identical spacers. One possible explanation, lending more credit to the idea of the creation of displacement damage in the substrate is that the lateral doping profiles are affected in different ways. Note that before irradiation, the series resistance is already different for the two splits. This could for example be related to the retrograde p-well and its interaction with the gate dielectric. While the NO oxide will retain the boron atoms in the surface, a more pronounced segregation could occur into the thermal oxide. This results then in a different vertical and lateral doping profile and, hence, series resistance. As a consequence, the interaction with the Frenkel pairs created by the high-energy protons will also be different in the two cases.

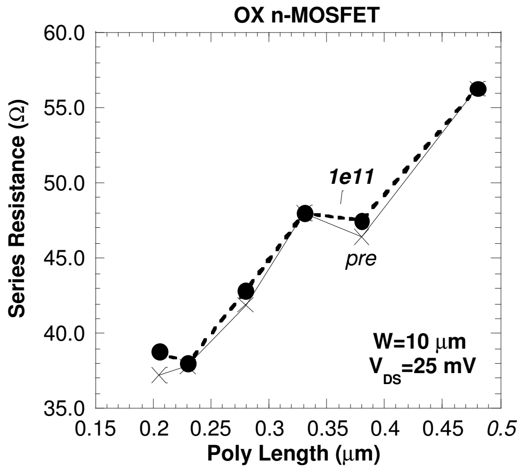

Fig. 9.a. Series resistance versus poly length for OX n-MOSFETs before and after a $3x10^{10}$ cm^{-2} 60 MeV proton irradiation.

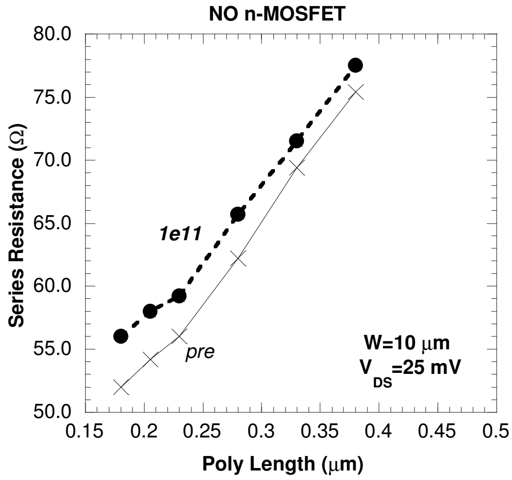

Fig. 9.b. Series resistance versus poly length for NO n-MOSFETs before and after a 10^{11} cm^{-2} 60 MeV proton irradiation.

E. GIDL Characteristics

Remains the issue of the uniformity of the damage along the channel, which has been raised in the foregoing. Unfortunately, the used test structures are not optimal for charge-pumping measurements. However, some information regarding the local damage near the drain can be gained from GIDL current measurements [19]-[20]. Figures 10 and 11 illustrate the behaviour for the L_{poly}=0.48 and 0.18 μm n-MOSFETs, respectively. The GIDL is measured from negative to zero gate voltage and corresponds with a drain voltage V_{DS}=25 mV and zero substrate bias V_{BS} in this case. In general, there is only a weak dependence on V_{BS}, measured in the range down to –2 V.

From the GIDL curves, one can again derive a stronger degradation for the NO transistors. While for the OX devices, it is mainly the slope of the GIDL curve which lowers after irradiation, there is also an unexpected shift to *positive* V_{GS} for NO. This would imply a net negative radiation-induced charge from oxide and interface traps, *close to the drain*. The latter fact is in contrast with the results from the normal input characteristics (see Table III for example). More work is needed to understand this inconsistency. From Fig. 10b, one can derive that for the normal operation (V_{GS}>-0.5 V) there is indeed a shift of the drain current to lower V_{GS}, in line with the V_T results. This is, however, not found for the 0.18 μm device. Note also the steeper subthreshold slope after irradiation for NO, while OX shows a reduction in the slope (Fig. 10a or 11a), pointing to the creation of interface traps close to the conduction band in the latter case.

In all devices studied, a (slight) reduction of the GIDL slope is observed in Figs 10 and 11. This indicates the creation of interface traps close to the valence band. A rebound of the GIDL curves is seen in addition, which confirms the rebound in V_T going from $3x10^{10}$ to 10^{11} p/cm^2. It is clear from these initial studies that the charge trapping in the NO oxides is more complex than expected and may show strong lateral non-uniformities.

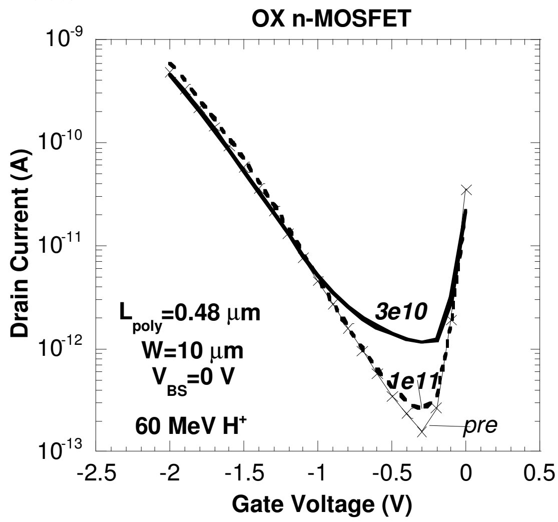

Fig. 10.a. GIDL current of a 0.48 μm OX n-MOSFET before and after exposure to a fluence of $3x10^{10}$ and 10^{11} 60 MeV p/cm^2. V_{DS}=25 mV.

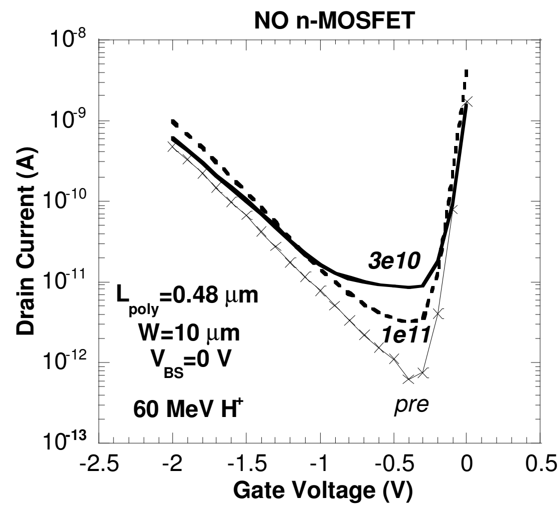

Fig. 10.b. GIDL current of a 0.48 μm NO n-MOSFET before and after exposure to a fluence of $3x10^{10}$ and 10^{11} 60 MeV p/cm^2. V_{DS}=25 mV.

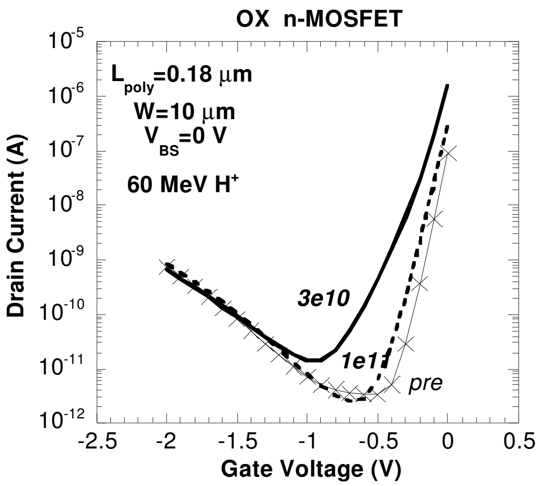

Fig. 11.a. GIDL current of a 0.18 μm OX n-MOSFET before and after exposure to a fluence of $3x10^{10}$ and 10^{11} 60 MeV p/cm^2. V_{DS}=25 mV.

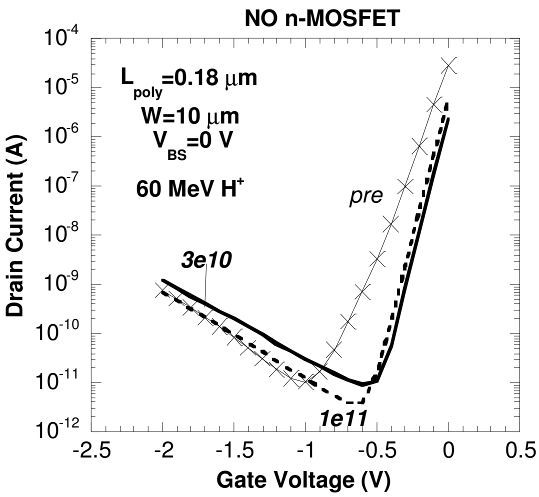

Fig. 11.b. GIDL current of a 0.18 μm NO n-MOSFET before and after exposure to a fluence of $3x10^{10}$ and 10^{11} 60 MeV p/cm^2. V_{DS}=25 mV.

In order to have a better understanding, additional characterisation, using e.g. low-frequency noise are desirable. Moreover, to come to a more detailed and quantitative picture of the degradation mechanisms and its length dependence, 2-dimensional numerical device simulations are indispensable. As qualitatively similar results have recently been obtained for IMEC's 0.13 μm CMOS transistors, corresponding with t_{ox}=2.0 nm, simulation efforts will be undertaken in the near future to address this point.

IV. Summary And Discussion

Summarising the above findings, it is clear that the degradation of 0.18 μm n-MOSFETs after 60 MeV proton irradiation shows a complex behaviour, whereby different mechanisms contribute. A possible model should enable to explain:

- the length dependence, whereby the shorter channels exhibit the strongest degradation
- the dependence on the gate dielectric
- the anomalous fluence dependence, which shows for most parameters a rebound for the highest fluence studied.

With respect to the first issue, it has been well-established in the past that the radiation induced changes in the V_T may show a strong length dependence [4],[21]-[23]. According to numerical simulations, this could be due to a more pronounced hole trapping in the oxide close to the drain [24]. In other words, the radiation-induced charge trapping and interface-state creation along the channel is not uniform, which yields a pronounced length-dependent device degradation. Using characterisation techniques, enabling a lateral profiling of the damage [25]-[27] has also concluded this. While the behaviour of the NO devices can be more or less understood in this context, the V_T cross-over observed for the OX transistors is less clear. A possible explanation is that in this case – and in particular for $3x10^{10}$ p/cm^2 – the impact of interface-state generation is higher for shorter L_{poly}.

In order to have a better view on the responsible degradation mechanisms, the classical charge separation method has been applied to the input curves of the transistors in the ohmic regime [28]. The effect of possible dopant deactivation effects described in [9]-[10] has been neglected here. Typical results for the areal density of induced interface (ΔN_{it}) and oxide traps (ΔN_{ot}) are given in Table III. From the data, one can derive that the NO devices show a much stronger charge trapping and higher interface state density than their OX counterparts. This points out the inferior quality of the NO dielectric used here, which was already demonstrated by the pre-rad results of Table IIa and IIb. In addition, the created oxide and interface charge increase with proton fluence. However, it is the balance between the two effects, which dictates the net V_T degradation.

TABLE III
RADIATION-INDUCED INTERFACE AND OXIDE TRAP DENSITY FOR THE n-CHANNEL TRANSISTORS

L_{poly} (μm) Gate	Fluence($x10^{10}$ p/cm^2)	ΔN_{it} (cm^{-2})	ΔN_{ot} (cm^{-2})
0.48(OX)	3	$0.7x10^9$	$1.8x10^9$
0.18(OX)	3	$17.1x10^9$	$5.6x10^9$
0.48(OX)	10	$2.3x10^9$	$3.9x10^9$
0.18(OX)	10	$12.5x10^9$	$8.1x10^9$
0.48(NO)	3	$-5.4x10^9$	$2.0x10^9$
0.18(NO)	3	$15.2x10^9$	$23.6x10^9$
0.48(NO)	10	$-263x10^9$	$266x10^9$
0.18(NO)	10	$260x10^9$	$267x10^9$

One can easily derive for example the ΔV_T cross-over behaviour for the OX devices, where ΔN_{it}>ΔN_{ot} for the shorter channel (0.18 μm), while the opposite holds for the long transistor (0.48 μm). The rebound behaviour is also explained readily from these data, both for NO and OX devices. Of course, one can wonder whether the standard charge separation technique still works properly for scaled, short-channel transistors. It should be reasonably well applicable for the longer device considered here. However, for the short-channel case, one should deal with the length-dependence of the subthreshold slope and the V_T (and possible radiation-induced changes). Additionally, the charge separation technique assumes a uniform lateral damage, which may not occur for the shortest devices. Nevertheless, the 0.18 μm data seem to be quite consistent with the 0.48 μm ones in Table III.

Note finally that the negative ΔN_{it} values for the long NO n-MOSFETs, which is in line with the reduction of the subthreshold swing, observed in Fig. 7b.

V. CONCLUSIONS

In conclusion, it has been shown that overall, NO n-MOSFETs show a more pronounced degradation after 60 MeV proton irradiation. This follows for example from the higher reduction of the threshold voltage and the higher increase in R_s. From a viewpoint of space applications, both processing splits show acceptable behaviour, i.e., hardness, since the magnitude of the observed changes is within acceptable levels. Nevertheless, a further process optimisation of the NO oxidation is necessary in order to achieve the same performance as the standard OX technology, both before and after irradiation. Such optimisation is certainly important with respect to further scaling to the 0.13-0.10 μm CMOS generations. Another surprising finding is that in spite of the thin gate dielectrics considered here, apparently severe charge trapping and interface-state creation occurs. This is especially true for the NO devices. Perhaps more worrying is the observed short-channel dependence of the degradation, which could point to a laterally non-uniform damaging of the near interface region. In the case of proton irradiation, one should consider defects at both sides of the interface, which could explain the complexity of the observed phenomena.

VI. ACKNOWLEDGMENTS

Guy Berger and his Colleagues of the Cyclone facility in Louvain-la-Neuve are warmly thanked for their assistance during the proton irradiations. This work has been performed within the frame of the ESTEC Work Order 11938/96/NL/NB. One of the Authors (A. Mercha) is indebted to the European Union for financial support within the frame of the TMR Network ENDEASD (ERB 4061 PL 97-0645).

VII. REFERENCES

[1] M. Khare, X.W. Wang, and T.P. Ma, "Transconductance in nitride-gate or oxynitride-gate transistors," *IEEE Electron Device Lett.,* vol. 20, pp. 57-59, Jan. 1999.

[2] G.J. Dunn and P.W. Wyatt, "Reoxidized nitrided oxide for radiation-hardened MOS devices," *IEEE Trans. Nucl. Sci.,* vol. 36, pp. 2161-2168, Dec. 1989.

[3] E.M. Vogel, W.L. Hill, V. Misra, P.K. McLarty, J.J. Wortman, J.R. Hauser, P. Morfouli, G. Ghibaudo, and T. Ouisse, "Mobility behavior of n-channel and p-channel MOSFET's with oxynitride gate dielectrics formed by low-pressure rapid thermal chemical vapor deposition," *IEEE Trans. Electron Devices*, vol. 43, pp. 753-758, May 1996.

[4] C. Claeys and E. Simoen, *Literature Study on Radiation Effects in Advanced Semiconductor Devices*, Report, P35284-IM-RP-0013, March 2000.

[5] M. Walters and A Reisman, "Radiation-induced neutral electron trap generation in electrically biased insulated gate field effect transistor gate insulators," *J. Electrochem. Soc.*, vol. 138, pp. 2756-2762, Sept. 1991.

[6] N.S. Saks, M.G. Ancona, and J.A. Modolo, "Generation of interface states by ionizing radiation in very thin MOS oxides," *IEEE Trans. Nucl. Sci.*, vol. 33, pp. 1185-1190, Dec. 1986.

[7] M. Ceschia, A. Paccagnella, A. Cester, A. Scarpa, and G. Ghidini, "Radiation induced leakage current and stress induced leakage current in ultra-thin gate oxides," *IEEE Trans. Nucl. Sci.*, vol. 45, pp. 2375-2382, Dec. 1998.

[8] M. Ceschia, A. Paccagnella, S. Sandrin, G. Ghidini, J. Wyss, M. Lavale, and O. Flament, "Low field leakage current and soft breakdown in ultra-thin gate oxides after heavy ions, electrons or X-ray irradiation," *IEEE Trans. Nucl. Sci*, vol. 47, pp. 566-573, June 2000.

[9] S.C. Witczak, R.C. Lacoe, M.R. Shaneyfelt, D.C. Mayer, J.R. Schwank, and P.S. Winokur, "Implications of radiation-induced dopant deactivation for npn bipolar junction transistors," *IEEE Trans. Nucl. Sci.*, vol. 47, pp. 2281-2288, Dec. 2000.

[10] S.C. Witczak, P.S. Winokur, R.C. Lacoe, and D.C. Mayer, "Charge separation technique for metal-oxide-silicon capacitors in the presence of hydrogen deactivated dopants," *J. Appl. Phys.*, vol. 87, pp. 8206-8208, June 2000.

[11] E. Simoen, A. Poyai, and C. Claeys, "The effect of substrate radiation-induced defects on the operation of deep submicron technologies," in the *Proc. of DECON 2001*, Eds B.O. Kolbesen, C. Claeys, P. Stallhofer, and F. Tardif, The Electrochem. Soc. Proc. vol. 2001-19, pp. 75-92, 2001.

[12] K. Hayama, H. Ohyama, K. Kobayashi, A. Poyai, E. Simoen, C. Claeys, Y. Takami, H. Takizawa, and A. Mohammadzadeh, in the *Proc. of the RADECS 2000 Workshop*, Louvain-la-Neuve, Belgium, 11-13 September, 2000, pp. 32-35.

[13] A. Poyai, E. Simoen, C. Claeys, K. Hayama, K. Kobayashi, and H. Ohyama, "Proton-irradiation effect on the electric-field enhancement of the generation lifetime in shallow p-n junction diodes," in the *Proc. of DECON 2001*, Eds B.O. Kolbesen, C. Claeys, P. Stallhofer, and F. Tardif, The Electrochem. Soc. Proc. vol. 2001-19, pp. 93-102, 2001.

[14] M. Da Rold, E. Simoen, S. Mertens, M. Schaekers, G. Badenes, and S. Decoutere, "Impact of gate oxide nitridation process on 1/f noise in 0.18 μm CMOS," *Microelectron Reliab.*, vol. 41, pp. 1933-1938, Dec. 2001.

[15] E. Simoen, J. Hermans, E. Augendre, T. Marescaux, C. Claeys, G. Badenes, and A. Mohammadzadeh, "Evidence for short-channel effect in the radiation response of 0.18 μm CMOS transistors," in the *Proc. of the RADECS 2000 Workshop*, Louvain-la-Neuve, Belgium, 11-13 September, 2000, pp. 25-31.

[16] Y. Taur, D.S. Zicherman, D.R. Lombardi, P.J. Restle, C.H. Hsu, H.I. Hanafi, M.R. Wordeman, B. Davari, and G.G. Shahidi, "A new "shift and ratio" method for MOSFET channel-length extraction," *IEEE Electron Device Lett.*, vol. 13, pp. 267-269, May 1992.

[17] J. Maimon and N. Haddad, "Overcoming scaling concerns in a radiation-hardened CMOS technology," *IEEE Trans. Nucl. Sci.*, vol. 46, pp. 1686-1689, Dec. 1999.

[18] J. Hermans, *Defect Engineering van Geavanceerde Materialen/ Componenten voor Ruimtevaarttoepassingen.* Masters Thesis, K.U. Leuven, 2000.

[19] A. Acovic, C.C.-H. Hsu, L.-C. Hsia, A. Balasinski, and T.-P. Ma, "Effects of X-ray irradiation on GIDL in MOSFETs," *IEEE Electron Device Lett.*, vol. 13, pp. 189-191, April 1992.

[20] N.C. Das, V. Nathan, R. Tallon, and R.J. Maier, "Radiation effects on gate induced drain leakage current in metal oxide semiconductor transistors," *J. Appl. Phys.*, vol. 72, pp. 4958-4962, Nov. 1992.

[21] J.S.T. Huang and J.W. Schrankler, "Flat-band voltage dependence on channel length in short-channel threshold model," *IEEE Trans. Electron Devices*, vol. 32, pp. 1001-1002, May 1985.

[22] J. Scarpulla, A.L. Amran, V.W. Gin, T.C. Morse, and K.T. Nakamura, "Gate size dependence of the radiation-produced changes in threshold voltage, mobility, and interface state density in bulk CMOS," *IEEE Trans. Nucl. Sci.*, vol. 39, pp. 1990-1997, Dec. 1992.

[23] M.R. Shaneyfelt, D.M. Fleetwood, P.S. Winokur, J.R. Schwank, and T.L. Meisenheimer, "Effects of device scaling and geometry on MOS radiation hardness assurance," *IEEE Trans. Nucl. Sci.*, vol. 40, pp. 1678-1685, Dec. 1993.

[24] V. Vasudevan and J. Vasi, "A two-dimensional numerical simulation of oxide charge buildup in MOS transistors due to radiation," *IEEE Trans. Electron Devices*, vol. 41, pp. 383-390, March 1994.

[25] W. Chen, A. Balasinski, and T.-P. Ma, "Lateral distribution of radiation-induced damage in MOSFETs," *IEEE Trans. Nucl. Sci.*, vol. 38, pp. 1124-1129, Dec. 1991.

[26] A. Balasinski and T.-P. Ma, "Ionizing radiation damage near CMOS transistor channel edges," *IEEE Trans. Nucl. Sci.*, vol. 39, pp. 1998-2003, Dec. 1992.

[27] A. Balasinski and T.-P. Ma, "Impact of radiation-induced nonuniform damage near MOSFET junctions," *IEEE Trans. Nucl. Sci.*, vol. 40, pp. 1286-1292, Dec. 1993.

[28] P.J. McWhorter and P.S. Winokur, "Simple technique for separating the effects of interface traps and trapped-oxide charge in metal-oxide-semiconductor transistors," *Appl. Phys. Lett.,* vol. 48, pp. 133-135, Jan. 1986.